Results in Materials 17 (2023) 100383

Contents lists available at ScienceDirect

Results in Materials

journal homepage: www.sciencedirect.com/journal/results-in-materials

Molecular dynamics simulations of cascade events in AlN☆

Michaela Kempner [a], Jesse M. Sestito [b], Yan Wang [a], Eva Zarkadoula [c,*,1]

[a] George W. Woodruff School of Mechanical Engineering, Georgia Institute of Technology, Atlanta, GA, 30332-0405, USA
[b] College of Engineering, Valparaiso University, Valparaiso, IN, 46383-6493, USA
[c] Materials Science and Technology Division, Oak Ridge National Laboratory, Oak Ridge, TN, 37831, USA

ARTICLE INFO

Keywords:
Molecular dynamics
Aluminum nitride
Radiation damage
Cascades

ABSTRACT

The radiation tolerance and the ability to retain its piezoelectric response make aluminum nitride (AlN) a good candidate for emerging sensing technologies in nuclear reactor environments. Furthermore, it has been shown that doping the ceramic with additional metals can further improve the piezoelectric response. Fundamental understanding of the response of AlN to radiation is important for ultimately improving the material's properties. In this paper, we use molecular dynamics and a recently developed interatomic potential fitted to defect energies to investigate low energy collision cascades in AlN. We additionally investigate the electronic stopping effect in the damage production for 20 keV Al ions. Our results show that for all energies the number of Al surviving defects is larger than that of N defects. Additionally, we find that even though the ballistic energy loss is the dominating mechanism, it is important to take into account the electronic stopping in order not to overestimate the number of defects.

1. Introduction

Emerging applications for sensors in extreme environments of nuclear reactors require the development of materials which are able to maintain their properties following radiation exposure. Piezoelectric sensors enable in situ acoustic/ultrasonic sensing for emerging nuclear energy concepts. Advanced piezoelectric sensors must exhibit good radiation response and maintain their piezoelectric response under radiation. Due to its electromechanical properties, aluminum nitride (AlN) is a good candidate material for piezoelectric devices, such as thin-film transducers [1–4]. Its radiation resistance to both neutron and gamma radiation and the ability to retain its piezoelectric response [5–7] makes AlN a promising candidate for use in ultrasonic transducers in environments with radiation exposure [8–12]. However, the mild piezoelectric response of AlN leads to a relatively low operating frequency of transducers [5]. Doping or co-doping AlN with metals has been shown to address the limitation of relatively small piezoelectric output [13]. Specifically, various Scandium (Sc) doping levels have been shown to enhance the piezoelectric response of AlN in experiments [14]. This implies that doped AlN compositions must also exhibit good radiation resistance and maintain their piezoelectric response after exposure to radiation. Recent *ab initio* calculations indicated that doping AlN with Sc can result in improved radiation response [15]. The design of new compositions of doped AlN that address current limitations of the piezoelectric behavior requires fundamental understanding to radiation at the atomistic level of the material response to irradiation.

Molecular dynamics (MD) modelling is a useful tool for investigating the primary radiation damage in materials [16]. Combined with visualization, MD simulations are especially helpful for understanding the defect formation in irradiated materials [17] at small time and length scales, often inaccessible by experiment. While there are multiple experimental studies on the radiation response of AlN, computational studies that can help acquire a fundamental understanding of the radiation damage in AlN are limited. Xi et al. [18] studied low-energy radiation effects in AlN using *ab initio* MD simulations, providing insights into the defect energetics, the defect effects in the electronic structure,

* Corresponding author.
E-mail address: zarkadoulae@ornl.gov (E. Zarkadoula).
[1] Current Affiliation: Center for Nanophase Materials Sciences, Oak Ridge National Laboratory, Oak Ridge, TN 37831.

https://doi.org/10.1016/j.rinma.2023.100383
Received 13 January 2023; Received in revised form 16 February 2023; Accepted 27 February 2023
Available online 1 March 2023

and the magnetic, electronic, and optical properties of AlN. Osektsy et al. [15] recently used *ab initio* calculations to investigate the electronic structure, configurations, formation, and binding energies of native and radiation induced point defects in pristine and Sc-doped wurtzite AlN. In the present paper, we use MD simulations and a recently developed modified embedded atom method (MEAM) potential [19] that was fitted to defect characteristics, to investigate the defect formation in AlN due to 5 keV, 10 keV, and 20 keV Al cascades. 20 keV cascades are run both with and without electronic stopping included so that the influence may be analyzed.

2. Methods

The Large-scale Atomic/Molecular Massively Parallel Simulator (LAMMPS) [20] is used for MD simulations. The Open Visualization Tool (OVITO) [21] is used for visualization. Wurtzite AlN is modelled with a semi-empirical MEAM force field [19], joined in this paper with the Ziegler-Biersack-Littmark repulsive potential [22] to account for short distance interactions, as described in the LAMMPS documentation [20]. The AlN system is generated in a simulation domain with periodic boundary conditions. For the 5 keV and 10 keV energy levels, the simulation domain has size 250 Å × 250 Å × 250 Å and contains about 1.472 million atoms. For the 20 keV energy level, the simulation domain has size 400 Å × 400 Å × 400 Å and contains about 6 million atoms. Prior to cascade simulations, the system energy is minimized under a zero anisotropic pressure and consequently the system is equilibrated for 20 ps under NPT dynamics with a 0.001 ps time step and with an isotropic zero pressure at 300 K. Cascades are performed by setting an Al atom as a primary knock-on atom (PKA) with an initial velocity corresponding to a kinetic energy of either 5 keV, 10 keV, or 20 keV [23]. For the case of 20 keV where the electronic stopping is taken into account, the mechanism is implemented as described in LAMMPS documentation [20]. The electronic stopping values were obtained using the SRIM (Stopping and Range of Ions in Matter) [22] software electronic stopping tables. The electronic stopping is applied to atoms with velocities corresponding to values larger than 12.4 eV kinetic energy [24–26]. For each of the four cases (5 keV, 10 keV, 20 keV, or 20 keV with electronic stopping), the PKA has a different initial velocity direction in each of ten single event cascades. The PKAs were chosen randomly, with the use of a random number generator to assign the PKA, choosing from the particle numbers that correspond to Al atoms. Each cascade progresses under NVE conditions with a variable timestep to account for the kinetics during the cascade evolution, ranging from 0.00001 to 0.001 ps. The cascade simulation time is 50 ps, to ensure that the system has cooled down. After each cascade, the Wigner-Seitz method [27] is used for defect analysis. The cluster identification is performed based on the second nearest neighbor criterion [28].

3. Results and discussion

To verify the force field, the Al threshold displacement energy was calculated without electronic stopping activated and compared to the previous *ab initio* calculations of Xi et al. [18]. The threshold displacement energy with an Al PKA was observed to be 122 eV for the [000$\bar{1}$] crystal direction. The threshold displacement energy with a N PKA was observed to be 119 eV for the [000$\bar{1}$] crystal direction. These energies closely approximate the *ab initio* value of 123 eV for Al and 112 eV for N [18]. These results indicate that the force field is suitable for modelling the displacement of ions within AlN.

The average and standard error of the number of Frenkel pairs (FPs) are illustrated in Fig. 1 (a) for the ten single event cascades at the 5 keV, 10 keV, and 20 keV PKA energy levels, and for 20 keV with electronic stopping. As expected, the average number of surviving defects increases with increasing PKA energy. The number of surviving FPs is smaller when the electronic stopping is activated than when it is not taken into account. To illustrate the damage range, in Fig. 1 (b) and 1(c) the surviving defects in a 20 keV Al cascade without and with electronic stopping are shown, respectively, for the same velocity direction. The frames have the size of the MD box (400 Å × 400 Å) and the (100) plane is shown in both cases.

The average and standard error of the number of FPs of defect type N and of defect type Al are illustrated in Fig. 2 (a) and (b) for the ten single event cascades at the 5 keV, 10 keV, and 20 keV PKA energy levels, and for 20 keV with electronic stopping. Regarding the correlation between the PKA energy and the surviving damage, the trends observed for each species agree with those observed for the total number of FPs. Even though the ratio of electronic energy loss to the nuclear energy loss is 0.25 for 20 keV Al ions in AlN, we observe that not taking the electronic stopping into account results in about 20% more FPs in all cases. This indicates that the process is important to consider even in relatively low energy cascade events resulting from PKA energies of a few tens of keV. In Fig. 2, we also observe that for all four cases, the numbers of surviving Al interstitials and Al vacancies are larger than the numbers of N interstitials and N vacancies, respectively. These results can be explained based on two observations. First, while for example the [000 $\bar{1}$] direction the threshold displacement energy for N is lower, it has been found [18] that the threshold displacement energies are dependent on the crystallographic directions. Additionally, the migration energies for N vacancies are lower than the ones for Al vacancies [19], meaning that N interstitial-vacancy recombination is enhanced, hence resulting in a

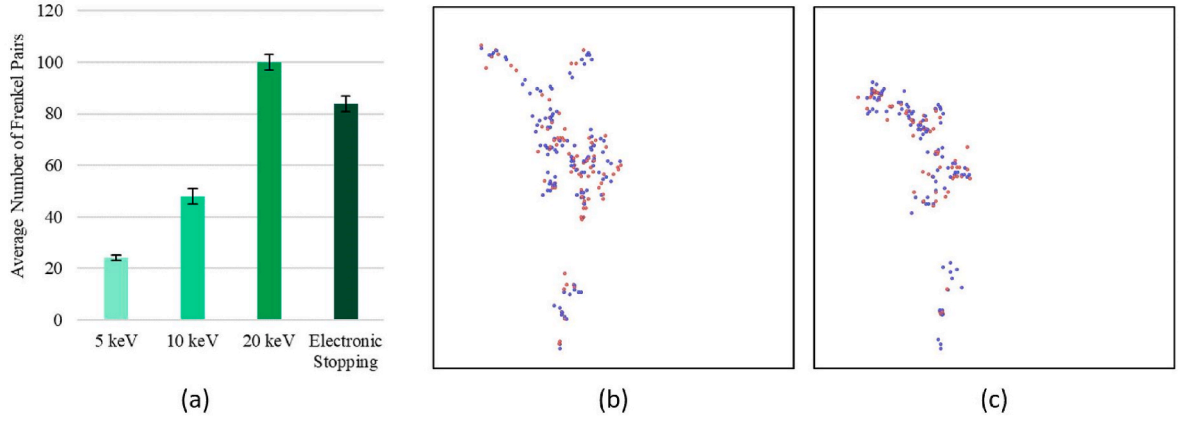

Fig. 1. (a) Average number, and standard error, of Frenkel pairs over ten single event cascades for the 5 keV, 10 keV, and 20 keV PKA energy levels, and for 20 keV with electronic stopping. (b) Surviving defects in a 20 keV Al cascade, without electronic stopping. (c) Surviving defects in a 20 keV Al cascade with electronic stopping. The same velocity direction as for (b) has been used. The frames have the size of the MD box (400 Å × 400 Å) and the (100) plane is shown in both cases. Al atoms are shown in blue and N atoms in red.

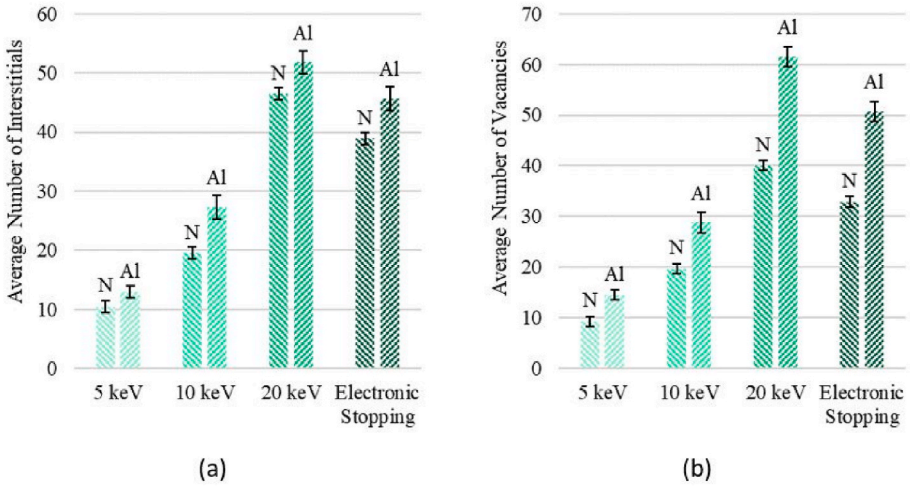

Fig. 2. (a) Average number, and standard error, of interstitials of type N and of type Al over ten single event cascades for the 5 keV, 10 keV, and 20 keV PKA energy levels, and for 20 keV with electronic stopping. (b) Average number, and standard error, of vacancies of type N and of type Al over ten single event cascades for the 5 keV, 10 keV, and 20 keV PKA energy levels, and for 20 keV with electronic stopping.

lower number of N defects.

To understand the lattice response to the cascades better, we additionally performed cluster analysis on the surviving defects. The total number of vacancy clusters of various sizes over ten single event cascades are illustrated in Table 1 for the 5 keV, 10 keV, 20 keV PKA energy levels, and for 20 keV with electronic stopping. Mostly isolated vacancies (point defects) and small clusters (size $\leq$3) are found, with the vacancy cluster count increasing with increasing energy. For the simulations with the electronic stopping, the cluster count is smaller compared to when the electronic stopping is ignored, which is relevant to the smaller overall number of FPs. For cluster size $\geq$4, more vacancy clusters are found when the electronic energy is considered, but because of the small count due to the relatively small energies these numbers do not differ significantly.

The total number of interstitial clusters of various sizes over ten single event cascades are illustrated in Table 2 for the 5 keV, 10 keV, and 20 keV PKA energy levels, and for 20 keV with electronic stopping. Similar to the vacancy clusters, mostly point defects and small clusters (size $\leq$3) are found, with the interstitial cluster count increasing with increasing energy, while the cluster count is smaller for the case with the electronic stopping activated. The largest interstitial cluster was of size 5 and was formed at the 20 keV PKA energy level. Overall, we observe that when the electronic stopping is incorporated in the number of defects is smaller and smaller clusters are formed. This is due to the fact that the electronic stopping, which is applied as friction term to moving atoms, slows down the atoms by removing energy, and therefore less energy is available for defect production. This energy removal through the friction term is reflected in the smaller number of defects and smaller clusters.

Table 1
Total number of vacancy clusters of various sizes over ten single event cascades for the 5 keV, 10 keV, and 20 keV PKA energy levels, and for 20 keV with electronic stopping.

Cluster Size	Number of Vacancy Clusters			
	5 keV	10 keV	20 keV	20 keV Electronic Stopping
1	132	268	542	448
2	35	57	128	100
3	5	13	45	31
4	4	10	11	16
5	1	2	3	6
6	0	0	1	2
7	0	2	0	1
8	0	0	0	0
9	0	0	2	0

Table 2
Total number of interstitial clusters of various sizes over ten single event cascades for the 5 keV, 10 keV, and 20 keV PKA energy levels, and for 20 keV with electronic stopping.

Cluster Size	Number of Interstitial Clusters			
	5 keV	10 keV	20 keV	20 keV Electronic Stopping
1	205	402	800	697
2	12	25	70	43
3	2	4	10	12
4	0	1	2	1
5	0	0	1	1

4. Conclusion

In this paper, MD simulations are used to examine the defect formation in AlN under due to 5 keV, 10 keV, and 20 keV Al cascades for the first time, using a recently developed interatomic potential. For 20 keV Al, cascades with and without electronic stopping were performed. Our results indicate that, for all energies, the number of Al defects is larger than the number of N defects. For 20 keV Al ions, even though the energy loss due to ballistic displacements dominates, with a ratio of electronic to nuclear energy loss of 0.25, we find that the surviving number of defects is about 20% larger when the electronic energy is ignored. It is also found that smaller numbers of point defects and small clusters are formed when the electronic stopping is considered in the simulations, while larger vacancy clusters may be formed when the electronic energy loss is ignored. AlN is an important functional material for various applications, from nuclear sensors to targeted property functionalization, where it is subject to interactions with ions. Therefore, better understanding of the atomic level processes for defect formation is important. Fundamentally understanding the exceptional response of this material to radiation conditions requires more computational studies at the atomistic levels, which can be enabled with newly developed force fields, such as the one used in this work [19] and a more recently developed potential that includes interactions with Sc dopants [29].

Credit author statement

Michaela Kempner: Conceptualization; Methodology; Investigation; Software; Formal analysis; Visualization; Writing – original draft;

Writing – review & editing, Jesse Sestito: Concept and results discussions; Validation; Writing – original draft, Yan Wang: Concept and results discussions; Writing – original draft; Funding acquisition, Eva Zarkadoula: Conceptualization; Methodology; Visualization; Supervision; Writing – original draft; Writing – review & editing; Funding acquisition; Project administration.

Declaration of competing interest

The authors declare that they have no known competing financial interests or personal relationships that could have appeared to influence the work reported in this paper.

Data availability

Data will be made available on request.

Acknowledgements

This work was supported in part by National Science Foundation under grant CMMI-1663227. EZ was supported by the Laboratory Directed Research and Development Program of Oak Ridge National Laboratory, managed by UT-Battelle, LLC, for the U. S. Department of Energy.

References

[1] Imrich Gablech, Jaroslav Klempa, Pekárek Jan, Petr Vyroubal, Hrabina Jan, Miroslava Holá, Jan Kunz, Brodský Jan, Pavel Neužil, Simple and efficient AlN-based piezoelectric energy harvesters, Micromachines 11 (2) (2020) 143.
[2] Hong Goo Yeo, Joontaek Jung, Minkyung Sim, Jae Eun Jang, Hongsoo Choi, Integrated piezoelectric aln thin film with SU-8/PDMS supporting layer for flexible sensor array, Sensors 20 (1) (2020) 315.
[3] Etienne Herth, Dame fall, jean-Yves Rauch, Virginie Mourtalier, and Grégory Guisbiers. "Thermal annealing of AlN films for piezoelectric applications, J. Mater. Sci. Mater. Electron. 31 (6) (2020) 4473–4478.
[4] Jiahao Zhao, Jun Han, Yanhui Xing, Wenkui Lin, Lun Yu, Xu Cao, Zheming Wang, Xin Zhou, Xiaodong Zhang, Baoshun Zhang, Fabrication and application of flexible AlN piezoelectric film, Semicond. Sci. Technol. 35 (3) (2020), 035009.
[5] B. Reinhardt, J. Daw, B.R. Tittmann, Irradiation testing of piezoelectric (aluminum nitride, zinc oxide, and bismuth titanate) and magnetostrictive sensors (remendur and galfenol), IEEE Trans. Nucl. Sci. 65 (1) (2017) 533–538.
[6] Brian T. Reinhardt, Andy Suprock, and Bernhard Tittmann. "Testing piezoelectric sensors in a nuclear reactor environment, in: AIP Conference Proceedings, vol. 1806, AIP Publishing LLC, 2017, p. 050005, no. 1.
[7] Hongbin Sun, Eva Zarkadoula, L. Miguel, Crespillo, William J. Weber, Vivek Rathod, Steven J. Zinkle, Pradeep Ramuhalli, Laser Doppler vibrometry for piezoelectric coefficient (d33) measurements in irradiated aluminum nitride, Sensor. Actuator.: Phys. 347 (2022), 113886.
[8] J. Daw, J. Rempe, J. Palmer, P. Ramuhalli, R. Montgomery, H.T. Chien, B. Tittmann, B. Reinhardt, P. Keller, NEET In-Pile Ultrasonic Sensor Enablement-Final Report. No. INL/EXT-14-32505, Idaho National Laboratory (INL), 2014.
[9] Joshua Daw, Joe Palmer, Pradeep Ramuhalli, Paul Keller, Robert Montgomery, Hual-Te Chien, Kohse Gordon, Bernhard Tittmann, Brian Reinhardt, Rempe Joy, Ultrasonic Transducer Irradiation Test Results. No. INL/CON-14-31882, Idaho National Lab.(INL), Idaho Falls, ID (United States), 2015.
[10] Pattrick Calderoni, David Hurley, Josh Daw, Austin Fleming, McCary Kelly, Innovative Sensing Technologies for Nuclear Instrumentation, in: 2019 IEEE International Instrumentation and Measurement Technology Conference (I2MTC), IEEE, 2019, pp. 1–6.
[11] Ben LaRiviere, Pradeep Ramuhalli, F. Kyle Reed, P.C. Joshi, M. Nance Ericson, Tolga Aytug, Miguel L. Crespillo, Steven J. Zinkle, William J. Weber, Eva Zarkadoula, Irradiation-induced degradation of surface acoustic wave devices fabricated on bulk AlN, in: IEEE Transactions on Device and Materials Reliability, 2022.
[12] B.R. Tittmann, B. Reinhardt, J. Daw, Introduction to special session on "ultrasonic transducers for harsh environments, in: AIP Conference Proceedings, vol. 1949, AIP Publishing LLC, 2018, p. 100001, no. 1.
[13] Sri Ayu Anggraini, Masato Uehara, Kenji Hirata, Hiroshi Yamada, Morito Akiyama, Effects of different divalent cations in mTi-based codopants (m= Mg or Zn) on the piezoelectric properties of AlN thin films, Ceram. Int. 46 (3) (2020) 4015–4019.
[14] Olaf Zywitzki, Thomas Modes, Stephan Barth, Hagen Bartzsch, Peter Frach, Effect of scandium content on structure and piezoelectric properties of AlScN films deposited by reactive pulse magnetron sputtering, Surf. Coating. Technol. 309 (2017) 417–422.
[15] Yuri Osetsky, Mao-Hua Du, Samolyuk German, Steven J. Zinkle, Eva Zarkadoula, Native and radiation induced point defects in AlN and Sc-doped AlN, Phys. Rev. Mater. (2022), 004600.
[16] Roger E. Stoller, Eva Zarkadoula. 1.20 - primary radiation damage formation in solids, in: Rudy J.M. Konings, Roger E. Stoller (Eds.), Comprehensive Nuclear Materials, second ed., Elsevier, 2020, ISBN 9780081028667, pp. 620–662.
[17] C.S. Becquart, Domain Christophe, Modeling microstructure and irradiation effects, Metall. Mater. Trans. 42 (4) (2011) 852–870.
[18] Jianqi Xi, Bin Liu, Yanwen Zhang, William J. Weber, Ab initio molecular dynamics simulations of AlN responding to low energy particle radiation, J. Appl. Phys. 123 (4) (2018), 045904.
[19] G.A. Almyras, Davide Giuseppe Sangiovanni, Kostas Sarakinos, Semi-empirical force-field model for the Ti1− xAlxN (0≤ x≤ 1) system, Materials 12 (2019) 215.
[20] Steve Plimpton, Fast parallel algorithms for short-range molecular dynamics, J. Comput. Phys. 117 (1) (1995) 1–19.
[21] Alexander Stukowski, Visualization and analysis of atomistic simulation data with OVITO–the Open Visualization Tool, Model. Simulat. Mater. Sci. Eng. 18 (2009) 015012.
[22] James F. Ziegler, Jochen P. Biersack, The stopping and range of ions in matter, in: Treatise on Heavy-Ion Science, Springer, Boston, MA, 1985, pp. 93–129.
[23] Eva Zarkadoula, Samolyuk German, Yanwen Zhang, William J. Weber, Electronic stopping in molecular dynamics simulations of cascades in 3C–SiC, J. Nucl. Mater. 540 (2020), 152371.
[24] J.M. Pruneda, Daniel Sánchez-Portal, Andrés Arnau, J.I. Juaristi, Emilio Artacho, Electronic stopping power in LiF from first principles, Phys. Rev. Lett. 99 (23) (2007), 235501.
[25] Eva Zarkadoula, Devanathan Ram, William J. Weber, M.A. Seaton, Ilian T. Todorov, Kai Nordlund, Martin T. Dove, Kostya Trachenko, High-energy radiation damage in zirconia: modeling results, J. Appl. Phys. 115 (8) (2014), 083507.
[26] Emilio Artacho, Electronic stopping in insulators: a simple model, J. Phys. Condens. Matter 19 (27) (2007), 275211.
[27] Kai Nordlund, M. Ghaly, R.S. Averback, M. Caturla, T. Diaz de La Rubia, J. Tarus, Defect production in collision cascades in elemental semiconductors and fcc metals, Phys. Rev. B 57 (13) (1998) 7556.
[28] Jarvis, Raymond Austin, Edward A. Patrick, Clustering using a similarity measure based on shared near neighbors, IEEE Trans. Comput. 100 (11) (1973) 1025–1034.
[29] Jesse M. Sestito, Michaela Kempner, Tequila AL. Harris, Eva Zarkadoula, Yan Wang, Development of aluminum scandium nitride molecular dynamics force fields with scalable multi-objective bayesian optimization, JOM (2022) 1–11.